

# Si wafer bonded of a-Si/a-SiNx distributed Bragg reflectors for 1.55-$\mu$m wavelength vertical cavity surface emitting lasers

Christophe Levallois, Alain Le Corre, Slimane Loualiche, Olivier Dehaese, Hervé Folliot, Cyril Paranthoen, Françoise Thoumyre, Christophe Labbé

▶ **To cite this version:**

Christophe Levallois, Alain Le Corre, Slimane Loualiche, Olivier Dehaese, Hervé Folliot, et al.. Si wafer bonded of a-Si/a-SiNx distributed Bragg reflectors for 1.55-$\mu$m wavelength vertical cavity surface emitting lasers. Journal of Applied Physics, 2005, 98 (4), pp.043107. 10.1063/1.2009075 . hal-00488055

**HAL Id: hal-00488055**
**https://hal.science/hal-00488055**

Submitted on 1 Jun 2010

**HAL** is a multi-disciplinary open access archive for the deposit and dissemination of scientific research documents, whether they are published or not. The documents may come from teaching and research institutions in France or abroad, or from public or private research centers.

L'archive ouverte pluridisciplinaire **HAL**, est destinée au dépôt et à la diffusion de documents scientifiques de niveau recherche, publiés ou non, émanant des établissements d'enseignement et de recherche français ou étrangers, des laboratoires publics ou privés.

# Si wafer bonded of a-Si/a-$SiN_x$ distributed Bragg reflectors for 1.55 µm wavelength vertical cavity surface emitting lasers.

C. Levallois, A. Le Corre, S. Loualiche, O. Dehaese, H. Folliot, C. Paranthoen, F. Thoumyre, and C. Labbé.

*Laboratoire d'Etude de Nanostructures Semiconductrices - CNRS UMR FOTON 6082*

*INSA de Rennes, 20 Avenue des Buttes de Coësmes, F34043 Rennes Cedex, France*

(Received

Amorphous silicon (a-Si) and amorphous silicon nitride (a-$SiN_x$) layers deposited by magnetron sputtering have been analyzed in order to determine their optical and surface properties. A large value of ~1.9 of index difference is found between these materials. Distributed Bragg reflectors (DBR) based on these dielectric materials quarter wave layers have been studied by optical measurements and confronted to theoretical calculations based on the transfer matrix method. A good agreement has been obtained between the experimental and expected reflectivity. A maximum reflectivity of 99.5% at 1.55 µm and a large spectral bandwidth of 800 nm are reached with only four and a half periods of a-Si/a-$SiN_x$. No variation of the DBR reflectivity has been observed with the time nor when annealed above 240°C and stored during few months. This result allows to use this DBR in a metallic bonding process to realize a vertical cavity surface emitting laser (VCSEL) with two dielectric a-Si/a-$SiN_x$ DBR. This bonding method using $AuIn_2$ as the bonding medium and Si substrate can be performed at a low temperature of 240°C without damaging the optical properties of the microcavity. The active region used for this VCSEL is based on lattice-matched InGaAs/InGaAsP quantum wells and a laser emission has been obtained at room-temperature on an optically pumped device.

PACS numbers: 81.15.Cd, 78.55.Qr, 42.55.Sa

## I. INTRODUCTION

Vertical cavity surface emitting lasers (VCSELs) operating at 1.55 µm are very attractive laser sources for low-cost telecommunication systems, especially in emerging metro fiber-optic networks. Their circular, spectral, and spatial single-mode beam provides very efficient fiber coupling. They also offer other advantages like wafer testing before packaging or fabrication in array configuration.[1] However, there are some obstacles to the realization of 1.55 µm monolithic VCSEL on InP substrate, such as a non-availability of lattice-matched high reflective Distributed Bragg Reflectors (DBRs). Attempts using material system such as InAlGaAs-InAlAs,[2] InAlGaAs-InP,[3] and AlGaAsSb-InP[4] have been used to realize lattice-matched DBRs on InP substrate, but most of these materials have a poor thermal conductivity.[1] Nevertheless, other methods have been developed to avoid this problem. Among these, 1.55 µm VCSELs have been fabricated using structures based on InP/InGaAsP optical microcavities fused to AlGaAs DBR.[5,6] This method allows to obtain continuous-wave (CW) operation thanks to good thermal properties of AlAs and GaAs materials.[1] However, high temperatures are necessary to operate wafer-fusion and the fusion bonded interface is located inside the microcavity, close to the active region. Therefore, a good surface preparation is required to ensure a high interface bonding quality. The hybrid technique consists of replacing the epitaxial mirror with DBR made of dielectric material which presents a high refractive index difference, such as $TiO_2$-$SiO_2$ or Si-$CaF_2$.[2,7] Consequently, a high reflectivity can be achieved with only few layer pairs. Moreover, their fabrication is easier and less expensive than DBR realized by epitaxial growth. However, to realize VCSELs with two efficient dielectric DBR, a bonding method is needed. An approach which can be employed consists in using a low temperature metallic bonding process.[8] Indeed, the high thermal conductivity of metals and a thin dielectric DBR can be an interesting way to reduce the overheating of the device under CW operation. Furthermore, the bonding interface is

formed outside the VCSEL cavity, which ensures a good interface quality between the active region and the dielectric Bragg mirrors.

In the present work, we report the fabrication and characterization of an original 1.55 µm wavelength dielectric DBR realized by magnetron sputtering. The dielectric materials used are amorphous silicon (a-Si) and amorphous silicon nitride (a-$SiN_x$). Such a dielectric DBR have been proposed for their potential applications in the infrared wavelength range,[9] but to our knowledge no work has been reported for a 1.55 µm wavelength VCSEL using this dielectric DBR. Though, the amorphous silicon is a very well known and extensively used material. The a-Si is low cost, highly pure, easy to sputter, and it presents an optical index with a large contrast with a-$SiN_x$. Moreover, the thermal conductivity for a-$SiN_x$ is higher than others dielectric materials ($SiO_2$ or $TiO_2$).[10] Thus the use of a-Si/a-$SiN_x$ as a bottom mirror is a promising candidate for a CW lasing operation of the VCSEL. Optical indexes and absorption coefficients of a-Si and a-$SiN_x$ have been studied to optimize the magnetron sputtering parameters. A Bragg mirror with these materials has been characterized by transmittance and reflectivity measurements. The reflectivity reaches a 99.5% value at 1.55 µm for four and a half periods and is confirmed by the simulation. A VCSEL cavity has been designed with two a-Si/a-$SiN_x$ Bragg mirrors, the sample being bonded on a Si substrate thanks to a metallic bonding process. $AuIn_2$ metal alloy is employed as the bonding medium and this method has been optimized for a low bonding temperature in order to reduce damages on dielectric DBR and InP based devices. This VCSEL has been characterized and laser emission has been obtained at room-temperature (RT).

## II. DIELECTRIC MATERIAL PROPERTIES

Prior to the metallic bonding and the final device fabrication, we have studied properties and optical parameters of a-Si and a-$SiN_x$. A magnetron sputtering system with

argon plasma is used to deposit films on a glass substrate. All the sputtered layers are realized on a plate cooled by water circulation. This method is low cost since a unique target of silicon is needed to obtain both a-Si and a-$SiN_x$ films. The introduction of nitrogen in the argon plasma leads to the formation of a-$SiN_x$. As we have no in situ control of the deposited layer, care has been taken to get reproducible deposit conditions. It implies a clean vacuum system (residual pressure in the $10^{-7}$ mbar range) and stable plasma conditions. Bulk layer have been studied. Deposit conditions are reproducible and measured optical constants remain stable when the samples stored in ambient air during six months and tested. Refractive indexes were determined by the simulation of optical transmission using the transfer matrix method (TMM)[11,12] and transmission measurements with a FTIR (Fourier Transform Infra-Red) spectrometer. Dispersion of the refractive index as a function of wavelength has been taken into account. A value near 3.74 has been found for the a-Si refractive index at 1.55 µm wavelength. This value is close to the ones found in literature[13,14] and is higher than crystalline Si value ($n$=3.45).[14] The a-$SiN_x$ refractive index depends on the nitrogen concentration in the plasma and the exact layer composition has not been measured. We have studied the $N_2$ flow rate influence on optical index with a total introduced gas pressure (Ar+$N_2$) of $10^{-2}$ Torr kept constant. As it is reported on Fig. 1, a large optical index variation from 1.83 to 3.74 can be obtained adjusting this parameter. Controlled plasma conditions are essential to obtain a-$SiN_x$ layers with a low optical index and a reproducible stoichiometry. These conditions require to work at high $N_2$ flow rates. The Fig. 1 clearly shows that the refractive index of a-$SiN_x$ is less sensitive to variations at high $N_2$ flow rates. With these conditions, the measured a-$SiN_x$ refractive index is close to 1.83. Consequently, a-$SiN_x$ presents a large optical index contrast (~1.9) with a-Si. The as deposited layer presents a good stability of its optical parameters with time. It shows no variations during six months of storage in an ambient air which is an indication of the insensitivity to moisture and to oxygen

incorporation. In addition, there is no need for auxiliary ion bombardment to reach good material quality with high compacity as it is required for oxygen based dielectric materials like $SiO_2$.

VCSEL operation is very sensitive to DBR losses which mainly come from scattering interface roughness or residual absorption. We have then characterized dielectric surface roughness by atomic force microscopy (AFM). Two layers of a-Si and a-$SiN_x$ have been deposited on InP substrates with quarter wavelength optical thicknesses. For the two samples, 1×1 $\mu m^2$ surface area have been scanned and AFM images obtained are represented in Fig. 2. By analyzing these images, the height distribution of each material have been extracted and represented in fig. 2(c). The root-mean-square surface roughness ($R_{rms}$) is obtained by the root-mean square calculation of the surface profile which is related to the width of the height distribution. The $R_{rms}$ deduced from these histograms are 1.1 nm and 1.6 nm for a-Si and a-$SiN_x$, respectively. These low roughness values ($R_{rms} \leq \lambda/1000$) ensure high surface quality and low scattering losses. Residual absorption in the DBR materials has been assessed. Amorphous silicon nitride is known for its low absorption in the infrared wavelength range[9] and this is confirmed by our optical transmission measurements: $\alpha_{a\text{-}SiNx} < 30\ cm^{-1}$. The same measurement on the quarter wavelength sample has been realized for a-Si layer with a thickness of ~1 μm and an absorption coefficient of about several hundreds of $cm^{-1}$ has been revealed. In order to accurately measure this residual absorption, several a-Si and a-$SiN_x$ layers were consecutively deposited to realize a Fabry-Perot microcavity on a glass substrate. This microcavity was designed for a resonant wavelength at 1.53 μm. It is composed of a λ/2 optical length of a-Si, sandwiched between two Bragg mirrors of 3.5 periods each. Such a structure has been simulated with TMM where the scattering losses have been ignored. The Fig.3 inset depicts the simulated transmission of the microcavity at the resonance wavelength versus the a-Si with no absorption for a-$SiN_x$ material. It reveals that the maximum

transmission observed is very sensitive to the a-Si residual absorption. Transmission is divided by a factor two when the a-Si absorption coefficient varies between 0 and 600 $cm^{-1}$. The simulated transmission spectrum has been compared with the FTIR measured spectrum (Fig. 3) and at the resonant wavelength a 390 ± 15 $cm^{-1}$ value is found for the a-Si absorption coefficient. This value is consistent with published values for amorphous silicon.[15] This rather high absorption is however counterbalanced by the large refractive index difference between a-Si and a-$SiN_x$. This large refractive index contrast yields a very short penetration depth for the optical mode, from the inner cavity into the Bragg mirror.[16] For this reason and because the total silicon thickness is small in the Bragg mirror, low losses by absorption are expected.

## III. DIELECTRIC DBR CHARACTERIZATION

A dielectric Bragg mirror with those materials has been realized and studied. The large refractive index contrast ensures a high reflectivity with only a few stacked layers. Four and a half periods of a-Si/a-$SiN_x$ are deposited on a glass substrate to realize a Bragg reflector with a resonant wavelength centered at 1.55 µm. This number of period have been determined by using the TMM and the optical parameters of dielectric materials in order to predict the smallest number of layers needed for the DBR to reach a high reflectivity (>99%). Furthermore, the first and the last material deposited during the DBR realization is a-Si. It allows to obtain a high refractive index difference for the two interfaces: air/DBR and DBR/glass substrate. Consequently, the periods number of the DBR is not an integer value. The computation gave optimum thicknesses of 103.6 nm for a-Si and 212.9 nm for a-$SiN_x$. The total thickness of this DBR is smaller than 1.4 µm. Optical characterizations were performed by FTIR transmittance and reflectance measurements using an uncooled Ge detector. As it is illustrated in Fig. 4, the position of the transmission minima is set at 1.55 µm, so the maximum reflectivity is expected to be near 1.55 µm. For this wavelength, the

transmittance is equal to 0.2%. A good agreement between calculated and measured spectra is obtained for the whole spectral range, and it shows that optical constants, thicknesses, and composition of each layer are well controlled and stays constants during sputtering deposition. The reflectivity of such a Bragg mirror has been computed using experimental material parameters as input values. The reflectivity obtained is greater than 99.5% at a center wavelength of 1.55 µm. A high reflectance value of R≥99.5% is obtained inside a spectral window greater than 100 nm centered around 1.55 µm. As illustrated in Fig. 5, a reflection measurement of this DBR mirror has been realized with a commercial FTIR spectrometer under an incidence angle of 27°. The reflectivity of the Bragg mirror has also been compared to a gold mirror reflectivity. These measures led to an evaluation of the experimental reflectivity situated between 99.2% and 99.6%. This result is in agreement with the reflectivity values deduced from the transmittance measurements. This measurement has been compared to a simulated spectrum. Due to the 27° optical incidence angle of the commercial spectrometer, the TE and TM polarizations of the incident ray have been taken into account in the TMM. As for transmittance measurements, a good agreement between the simulated and measured spectrum is reached, as it is seen in Fig. 5. In order to obtain the 3 dB spectral bandwidth, simulations were performed above the germanium detector cut off wavelength. A spectral bandwidth larger than 800 nm is deduced from this simulation.

## IV. DOUBLE DIELECTRIC DBR VCSEL FABRICATION

Other reflectivity measurements have been realized to verify the stability and aging properties of the Bragg mirror at RT when stored in air ambient for a duration of three months. No variation of the mirror properties have been observed. The mirror is also found to be very stable when it was annealed up to 240°C. This stability of the mirror reflectivity with temperature allowed us to bond it to a silicon substrate with a fused metallic layer. A first five

and a half periods a-Si/a-$SiN_x$ DBR has been deposited on an active region. This active region, grown by molecular beam epitaxy (MBE), is a 1.5λ cavity containing multi quantum wells GaInAs/GaInAsP and will be described in details in the following part. As it is reported in the Fig. 6 inset, this Bragg mirror becomes the bottom mirror of the VCSEL cavity at the end of the process. On top of this first Bragg mirror, a 50 nm thick titanium followed by a 500 nm thick gold layers were deposited by electron-beam evaporation. The same operation is realized on a silicon substrate. The thin titanium layer is used to allow a better adhesion of the gold layer. This step is followed by the deposition of an indium layer on the 1×1 $cm^2$ sample area by thermal evaporation. The sample and the silicon substrate are joined together. Thus, the indium layer is sandwiched between the two gold layers. A pressure close to 5 $kg.cm^{-2}$ is applied during the annealing process to ensure intimate contact between the Si substrate and the sample. Above 157°C, the indium layer melts, and an interdiffusion takes place between Au and In. According to the Au-In phase diagram, when In melts and wet the adjacent Au layers, a Au-In alloy is formed. If the temperature is held above 200°C, In melts and breaks up the $AuIn_2$ layers to form a mixture of liquid and solid, then forms more $AuIn_2$. The solid-liquid interdiffusion continues until the mixture solidifies. It seems this step is followed by a solid state diffusion to form a mixture of AuIn and $AuIn_2$ as has been viewed by other authors.[17] In our case, the annealing is realized with a furnace set at a temperature of 260°C in a clean room normal atmosphere. The highest temperature reached by the sample after 20 minutes annealing is 240°C. Once the bonding between the Si substrate and the dielectric DBR is completed, the InP substrate is removed prior to the deposition of the front DBR. The InP substrate is first reduced to about 80 µm by mechanical polishing. Finally, the remaining InP is completely removed by a selective chemical etching using a mixture of HCl and $H_3PO_4$ and an InGaAs stop etch layer. This last layer is removed by an other selective etching solution to reach the inner cavity. This process is followed by the deposition of the second

DBR which consists in five periods a-Si/a-$SiN_x$ mirror (Fig. 6). This microcavity has been characterized by reflectivity measurement. Under an angle of 27°, the simulated and experimental microcavity spectra reported in Fig. 6 are in excellent agreement. Thus, this result clearly indicates that the optical properties of the microcavity and the reflectivity of the bottom mirror have not been damaged by the metallic bonding process. A resonant wavelength is observed at 1.51 µm for the experimental configuration. For normal incidence, this resonant wavelength is shifted to a longer wavelength and simulated reflectivity give a resonant wavelength of 1.53 µm. This deviation from the designed resonant wavelength of 1.55 µm can be explained by the thickness of InGaAsP material which is 6.5% lower than nominal values. This results, obtained by X ray characterization after realization of the active region, implies a cavity length shorter than the one expected.

## V. VCSELs DESIGN AND CHARACTERIZATION

The active region, grown by MBE, has an optical length of 1.5λ and contains three active zones of seven InGaAs/InGaAsP quantum wells (QWs). Lattice-matched alloy ($In_{0.8}Ga_{0.2}As_{0.435}P_{0.565}$) is used as a barrier and each active zone is separated by InP layers. In order to obtain an efficient optical pumping absorption, each group of seven QWs is sandwiched between quaternary barriers of controlled thicknesses. This design of the active region allows to obtain an homogenous optical absorption of the pump power and then an homogenous carrier injection.[18] The photopumping experiment consists in focusing a laser beam with a microscope objective (×10) on the front mirror of the VCSEL with a spot diameter of 10 µm. The laser emission is collected back by the same objective and transmitted through a beam splitter. The signal is injected in a large core diameter optical fiber connected to a spectrum analyzer. The photopumping of the active region is realized by a pulsed Q-switched YAG laser at 1.064 µm wavelength. The constant pulse width is 1 ns with a

repetition rate of 6.6 kHz. The average signal emitted by the VCSEL versus the peak power of the pump is reported in Fig. 7. A laser emission has been observed at RT and the laser spectrum for the threshold value is reported in the inset of the figure with an emission wavelength of 1.513 µm. This emission wavelength is shorter than the expected one and it is in agreement with the FTIR measurements. The threshold is reached for a 500 mW pump peak power. This value has been corrected by the reflection of the top mirror at 1.064 µm. However, the optical pump pulse width of 1 ns is equivalent to photoluminescence decay time of the InGaAs QWs.[19] Thus, the pumped active region does not reach its steady state within a pulse duration and the threshold value is given as an indication. Nevertheless, this measurement can be considered as a preliminary characterization of the device in order to show that a laser emission could be reached. Several optimizations will be carried out in the near future, like the fine tuning between the resonant wavelength of the cavity and the maximum optical gain of the QWs.

## VI. CONCLUSION

Optical properties of a-Si and a-$SiN_x$ sputtered dielectric layers have been studied. These materials present a high surface quality with a low roughness as controlled by AFM measurement. A large optical index difference of ~1.9 at 1.55 µm is found between these materials. A high quality Bragg mirror composed of these dielectric layers has been realized and tested. A reflectivity of 99.5% at 1.55 µm optical telecommunication wavelength and a very large spectral bandwidth of 800 nm for a four and a half a-Si/a-$SiN_x$ stack of $\lambda/4$ thickness has been demonstrated. The annealing up to 240°C or the storage of the mirror during few months at RT in air ambient seems to indicate good aging properties with time and temperature. In order to obtain a VCSEL with two dielectric DBRs, a low temperature metallic bonding process (240°C) on silicon substrate has been used without damaging the

optical properties of the device. The device optically pumped shows a laser emission at room temperature.

## ACKNOWLEDGMENTS

The authors wish to thank the Britain region for supporting this project.

## References


[1] Karim, S. Björlin, J. Piprek, and J. E. Bowers, IEEE J. Select. Topics in Quantum Electron. **6**, 1245 (2000).

[2] D. Sun, W. Fan, P. Kner, J. Boucart, T. Kageyama, R. Pathak, D. Zhang, and W. Yuen, IEEE Photon. Technol. Lett. **15**, 1677 (2003).

[3] J. Boucart, R. Pathak, D. Zhang, M. Beaudoin, P. Kner, D. Sun, R. J. Stone, R. F. Nabiev, and W. Yuen, IEEE Photon. Technol. Lett. **15**, 1186 (2003).

[4] G. Almuneau, E. Hall, T. Mukaihara, S. Nakagawa, C. Luo, D. R. Clarke, and L. A. Coldren, IEEE Photon. Technol. Lett. **12**, 1322 (2000).

[5] A. Karim, P. Abraham, D. Lofgreen, Y. J. Chiu, J. Piprek, and J. Bowers, Appl. Phys. Lett. **78**, 2632 (2001).

[6] A. Syrbu, A. Mircea, A. Mereuta, A. Caliman, C. A. Berseth, G. Suruceanu, V. Iakovlev, M. Achtenhagen, A. Rudra, and E. Kapon, IEEE Photon. Technol. Lett. **16**, 1230 (2004).

[7] R. Shau, H. Halbritter, F. Riemenschneider, M. Ortsiefer, J. Rosskopf, G. Böhm, M. Maute, P. Meissner, and M. C. Amann, Electron. Lett. **39**, 1728 (2003).

[8] H. C. Lin, W. H. Wang, K. C. Hsiek, and K. Y. Cheng, Electron. Lett. **38**, 516 (2002).

[9] D. I. Babic, J. J. Dudley, M. Shirazi, E.L. Hu, and J. E. Bowers, J. Vac. Sci. Technol. A. **9**, 1113 (1991).

[10] J. Piprek, H. Wenzel, H.-J. Wünsche, D. Braun, and F. Henneberger, Proc. of the SPIE Int. Society for Optical Engineering 2399, 605 (1995).

[11] J. B. Pendry and A. MacKinnon, Phys. Rev. Lett. **69**, 2772 (1992).

[12] P. M. Bell, J. B. Pendry, L. M. Moreno, and A. J. Ward, Comput. Phys. Comm. **85**, 306 (1995).

[13] G. K. Hubler, C. N. Waddell, W. G. Spitzer, J. E. Fredrickson, S. Prussin, and R. G. Wilson, J. Appl. Phys. **50**, 3294 (1979).

[14] C. N. Waddell, W. G. Spitzer, J. E. Fredrickson, G. K. Hubler, and T. A. Kennedy, J. Appl. Phys. **55**, 4361 (1984).

[15] B.S. Richards, A.B Sproul, and A. Lambertz, *Optical Characterisation of Sputtered Silicon Thin Film on Glass*, 2nd World Conf. and Exhibition on Photovoltaic Solar Energy Conversion, (1998).

[16] D. I. Babic, Y. Chung, N. Dagli, and J. E. Bowers, IEEE J. Quantum. Electron. **29**, 1950 (1993).

[17] C. C. Lee, C. Y. Wang, and G. Matijasevic, IEEE Trans. Comp. Hybrids. Manuf. Technol. **16**, 311 (1993).

[18] J. Geske, K. G. Gan, Y. L. Okuno, J. Piprek, and J. E. Bowers, IEEE J. Quantum. Electron. **40**, 1155 (2004).

[19] P. Michler, A. Hangleiter, A. Moritz, V. Härle, and F. Scholz, Phys. Rev. B. **47**, 1671 (1993).

**Figures captions**

**Figure 1**

Refractive index versus nitrogen flow rate for a total pressure ($Ar+N_2$) of $10^{-2}$ Torr kept constant. The circles show the experimental data and the solid curve is a guide for the eyes.

**Figure 2**

Surfaces AFM images ($1\times1$ $\mu m^2$) of a-Si (a) and a-$SiN_x$ (b) with quarter wavelength optical thicknesses deposited on InP. (c) Histogram of height distribution extracted by the analysis of AFM images.

**Figure 3**

Transmittance of a-Si microcavity realized with two a-Si/a-$SiN_x$ DBR of 3.5 periods each deposited on a glass substrate. The insert shows the simulated transmittance of such a filter at the 1.55 µm resonant wavelength versus the absorption coefficient of the a-Si layers.

**Figure 4**

Simulated and measured transmittance of 4.5 periods a-Si/a-$SiN_x$ DBR deposited on a glass substrate.

**Figure 5**

Simulated and measured reflectivity of a-Si/a-$SiN_x$ DBR of 4.5 periods deposited on a glass substrate under an incidence angle of 27°. The insert shows the details of the spectra between 1.5 µm and 1.6 µm wavelength.

**Figure 6**

Simulated and measured reflectivity of the VCSEL realized after metallic bonding process. The schematic diagram of the device tested is represented on the figure.

**Figure 7**

Average power emitted by the VCSEL versus the peak power of the optical pump. The insert shows the laser spectrum near the threshold value.

**FIG. 1.**



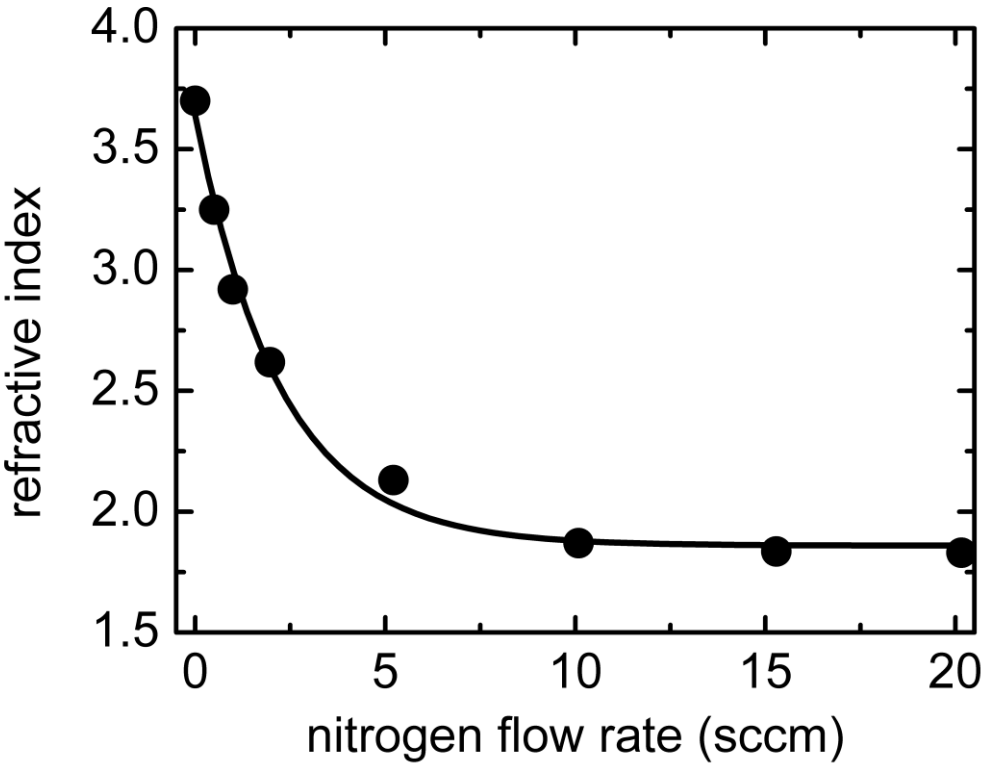

4.0
3.5
3.0
2.5
2.0
1.5
refractive index
0
5
10
15
20
nitrogen flow rate (sccm)

**FIG. 2.**



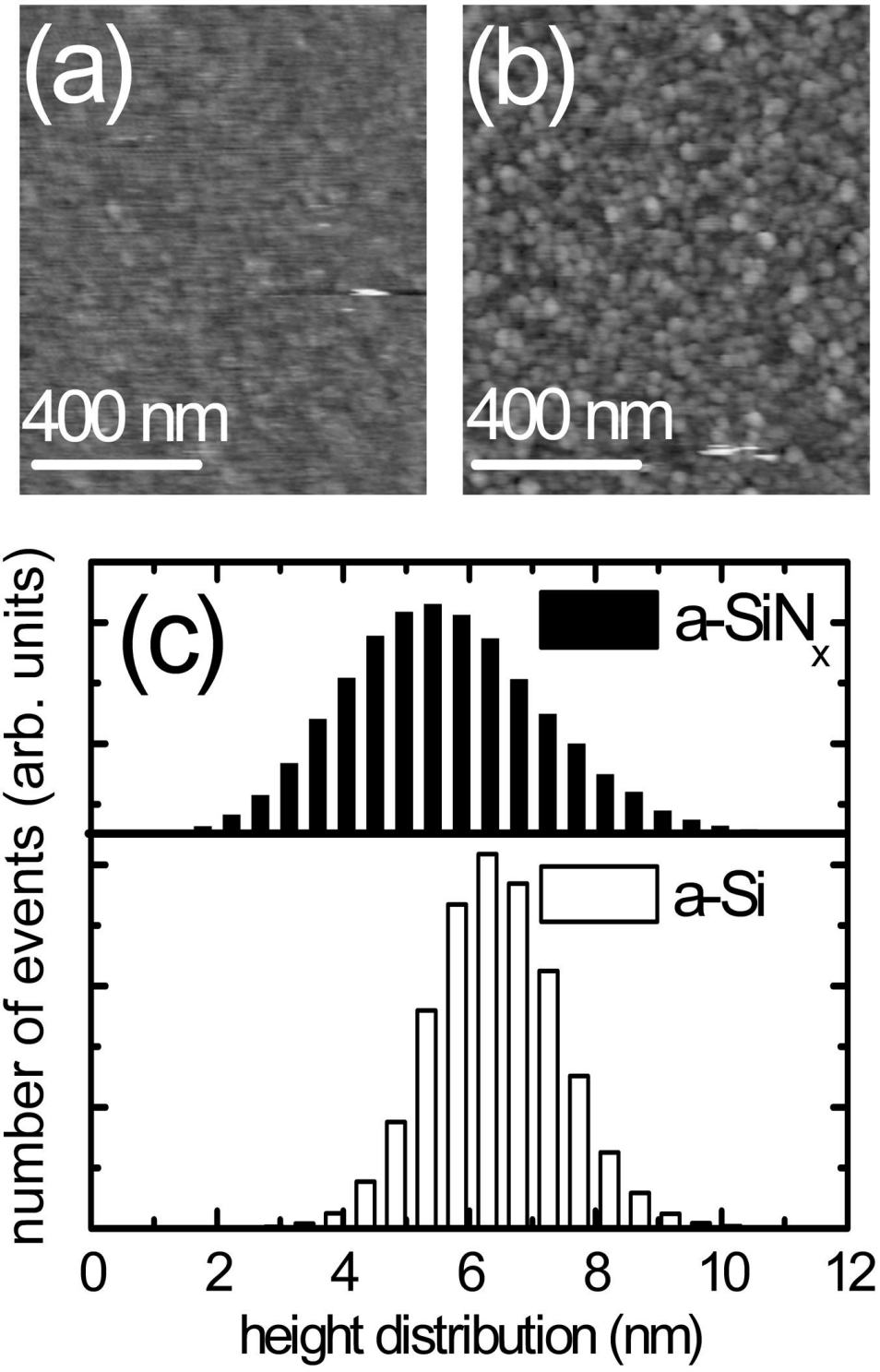

(a)
400 nm
(b)
400 nm
(c)
a-SiN$_x$
a-Si
number of events (arb. units)
0
2
4
6
8
10
12
height distribution (nm)

**FIG. 3.**



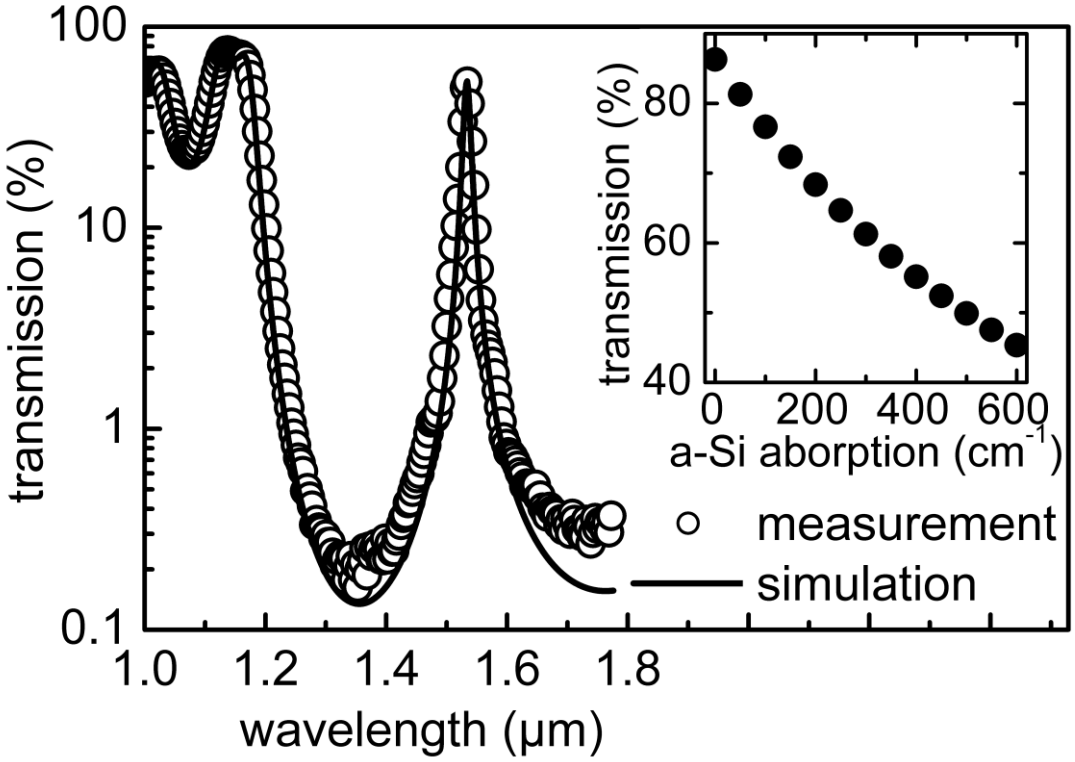

100
10
1
0.1
transmission (%)
1.0
1.2
1.4
1.6
1.8
wavelength (μm)
measurement
simulation
80
60
40
transmission (%)
0
200
400
600
a-Si aborption (cm-1)

**FIG. 4.**



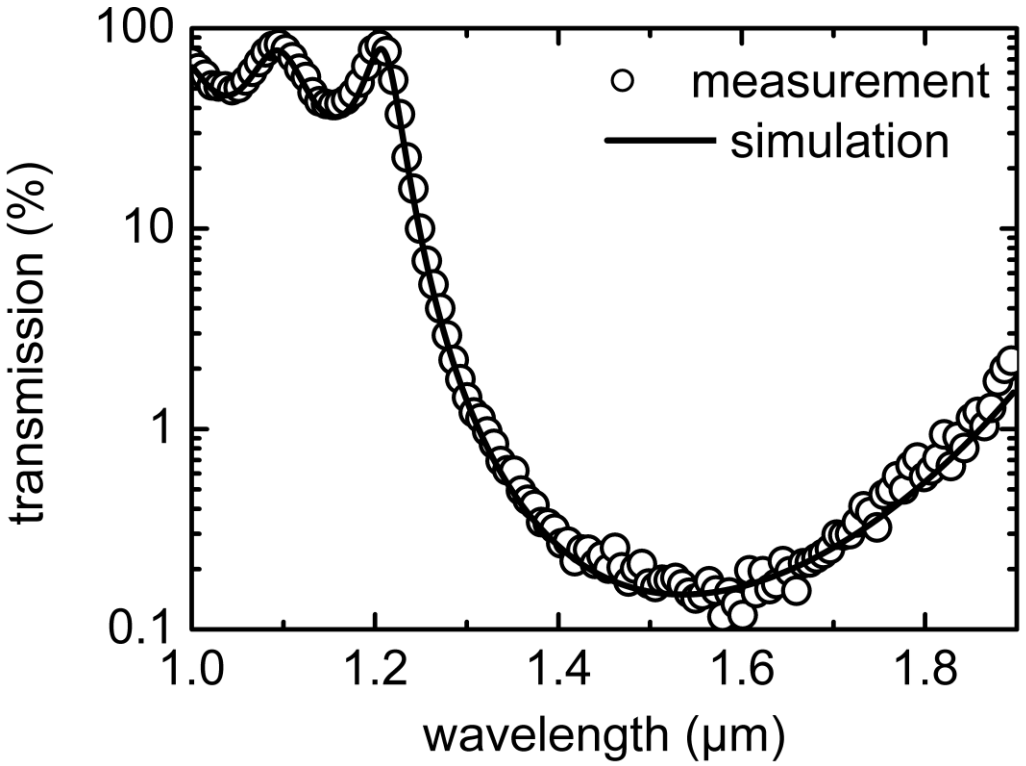

100
10
1
0.1
transmission (%)
1.0
1.2
1.4
1.6
1.8
wavelength (μm)
measurement
simulation

**FIG. 5.**



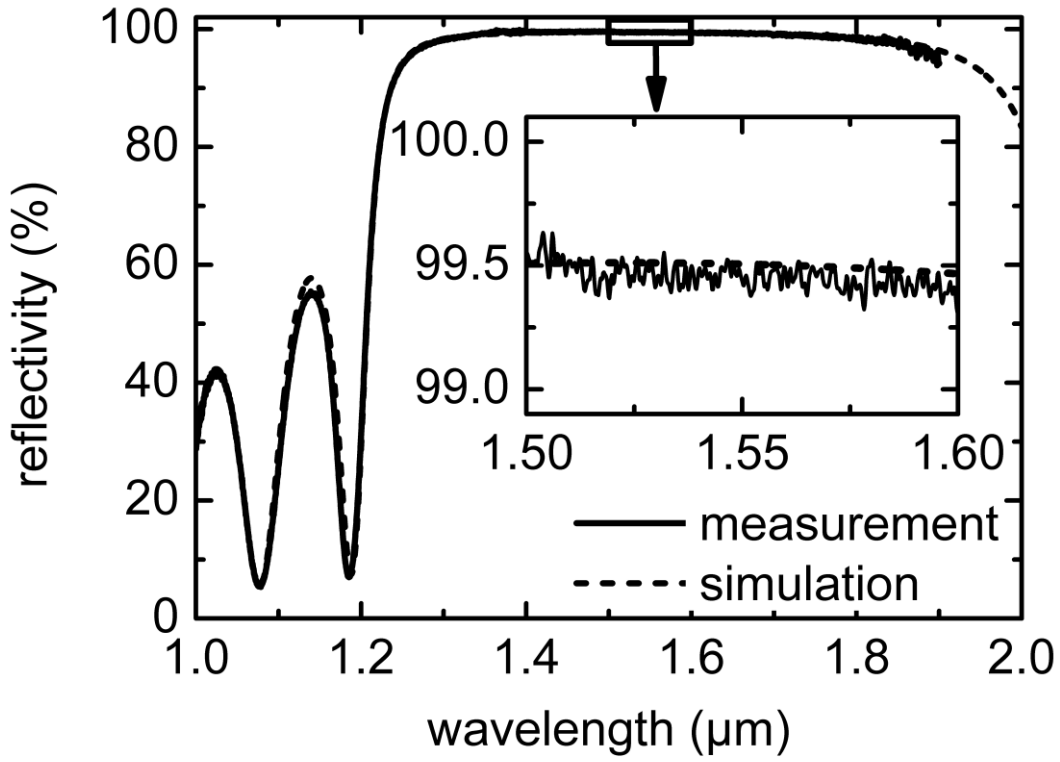

reflectivity (%)
wavelength (μm)
100
80
60
40
20
0
1.0
1.2
1.4
1.6
1.8
2.0
100.0
99.5
99.0
1.50
1.55
1.60
measurement
simulation

**FIG. 6.**



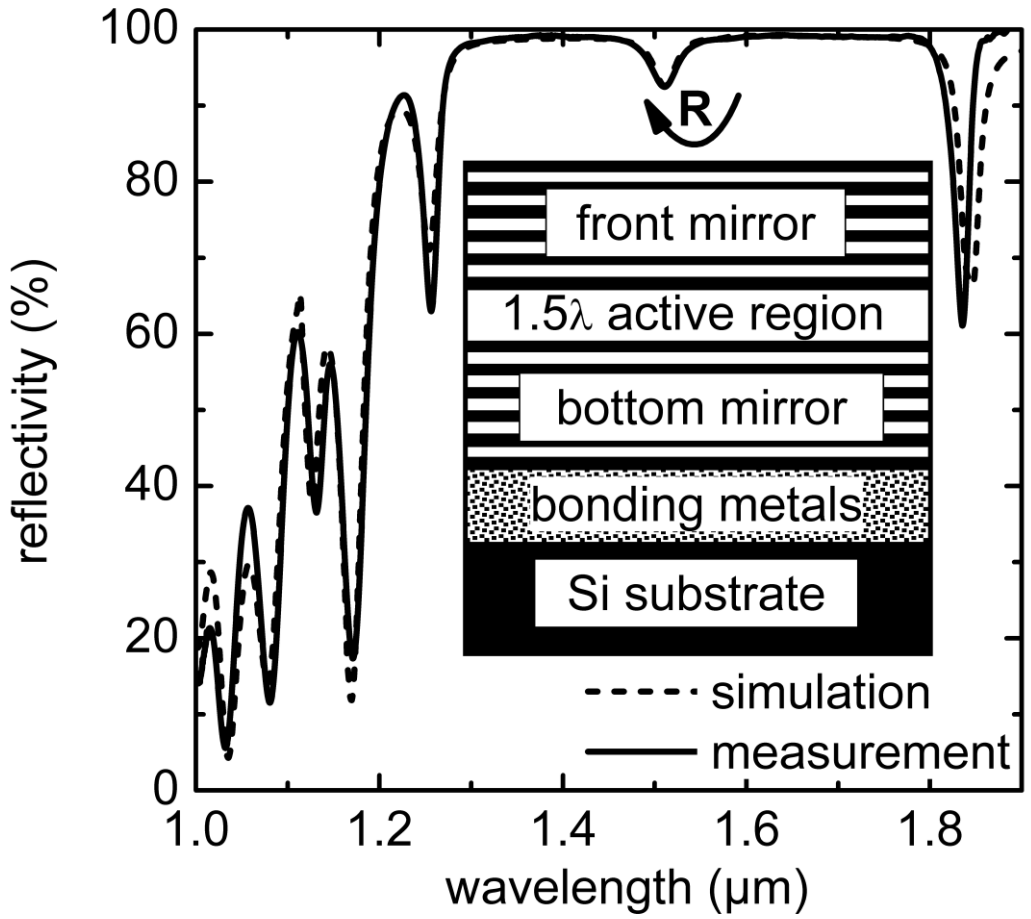
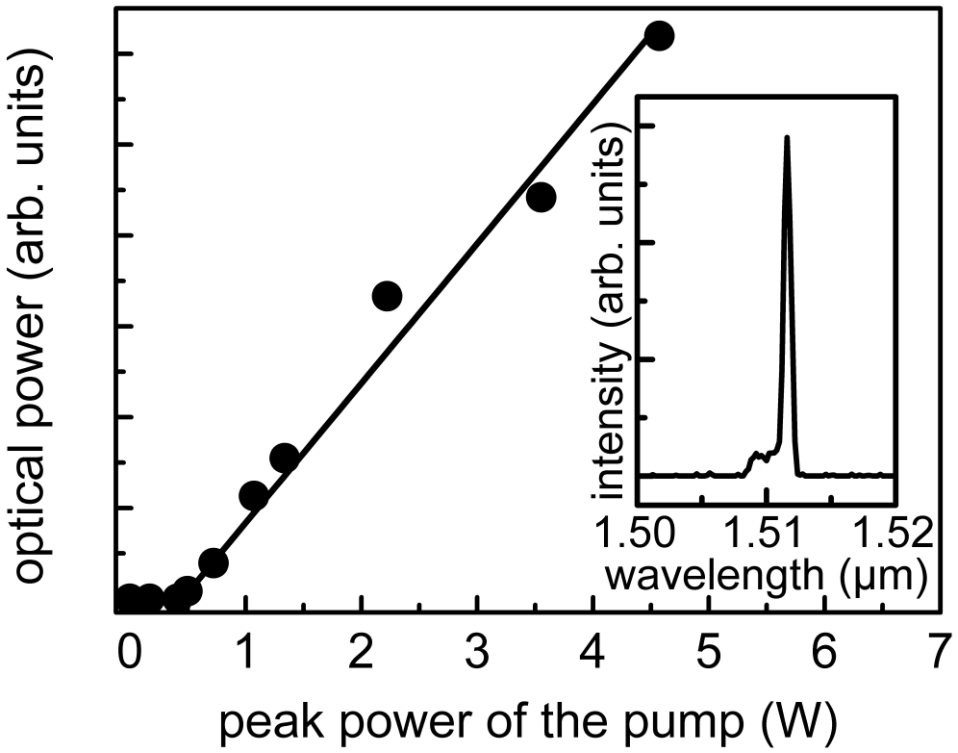

100
80
60
40
20
0
reflectivity (%)
1.0
1.2
1.4
1.6
1.8
wavelength (μm)
R
front mirror
1.5λ active region
bottom mirror
bonding metals
Si substrate
simulation
measurement

**FIG. 7.**




optical power (arb. units)
peak power of the pump (W)
0
1
2
3
4
5
6
7
intensity (arb. units)
1.50
1.51
1.52
wavelength (μm)